NANO LETTERS

2006
Vol. 6, No. 9
1973−1976

A Nanofluidic Railroad Switch for DNA

Robert Riehn,*,†,‡,§ Robert H. Austin,† and James C. Sturm‡

Department of Physics and Department of Electrical Engineering, Princeton University, Princeton, New Jersey 08544

Received May 18, 2006; Revised Manuscript Received July 2, 2006

ABSTRACT

We present a metamaterial consisting of a two-dimensional, asymmetric lattice of crossed nanochannels in fused silica, with channel diameters of 80 nm to 140 nm. When DNA is introduced, it is stretched and linearized. We show that the asymmetry in channel dimensions gives rise to a preferred direction for DNA orientation and a preferred direction for transport under dc electrophoresis. Interestingly, the preferred axis of orientation and transport can be switched by 90° through application of an ac voltage. We explain the results in terms of an energy landscape for polyelectrolytes that consists of entropic and dielectrophoretic contributions and whose strength and sign can be tuned by changing the ac field strength.

Polymer science was revolutionized by de Gennes,[1] Edwards,[2] and others, who put forward nanometer-scale models of interacting and confined polymer chains to explain the properties of bulk polymers, polymer melts, and polymer solutions. Experimental verification of these nanometer-scale models is now becoming feasible as nanofabrication is approaching the scale of the persistence length of polymers, such as DNA.[3−9] While previous authors studied one-dimensional or isotropic two-dimensional systems, we have investigated a two-dimensional metamaterial made of an asymmetric lattice of nanochannels.

The asymmetric lattice is formed by orthogonally intersecting two arrays of nanochannels that have equal pitch, but dissimilar channel cross sections (Figure 1). For our experiments, we interfaced a stripe of the metamaterial to two microfluidic channels, such that voltages could be applied at a 45° angle to both principal directions of the two-dimensional structure. We show that in this array of channels and junctions, electrophoresis transports DNA in a fashion somewhat similar to the Pockels effect[10] in optics, in as far as the transport is anisotropic, and the anisotropy can be switched by applying an ac voltage codirectional with the driving dc voltage. We will explain how this effect arises from an interplay of entropic and dielectrophoretic energy contributions close to the nanochannel junctions. Our discussion builds on the concepts developed for straight nanochannels, and expands these concepts to DNA at nanochannel junctions, symmetric and asymmetric, the distribution of electric fields in such structures, and the impact of ac fields on DNA in a complex nanofluidic environment.

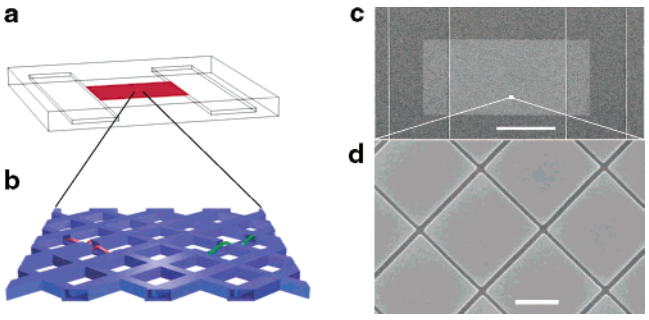

Figure 1. Schematic of the device and scanning electron microscopy (SEM) micrographs of structures before sealing the fluidic system. (a) Schematic overview of the device, which consists of one microchannel each on the left and the right, both 100 μm wide and 1 μm deep, linked by a 200 μm long and 120 μm wide nanofluidic region. (b) Enlarged schematic of the nanofluidic region, consisting of a square lattice of nanochannels, with differing channels widths along the principal axes. The green DNA molecule is confined to a wide channel, as in the case of a purely dc field. The red DNA molecule is confined to a narrow channel, and corresponds to a molecule that is subject to an appropriate ac voltage. (c) Overview SEM micrograph of a device used in this publication. (d) SEM micrograph of the local structure, showing a lattice with 2 μm period, and nanochannel widths of 100 and 140 nm, respectively. During transport measurements, the electric field was applied horizontally in this figure.

The effects of anisotropic transport and switching of the transport direction are demonstrated in Figure 2. A λ-DNA molecule was observed moving along the direction of the wider channels when only a dc bias was applied between the microchannels. The molecule was stretched out and aligned with the wide channels, at an angle to the direction of the externally applied field. However, when an ac voltage was added to the dc bias, the DNA molecule aligned along

* Corresponding author. Phone: +1-609-258-3158. Fax: +1-609-258-1115. E-mail: rriehn@princeton.edu.
† Department of Physics, Princeton University.
‡ Department of Electrical Engineering, Princeton University.
§ Present address: Physics Department, North Carolina State University, Raleigh, NC 27695.

10.1021/nl061137b CCC: $33.50
Published on Web 08/08/2006

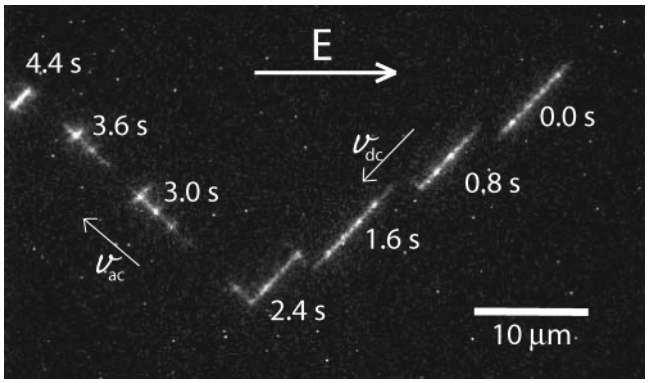

Figure 2. λ-DNA moving through the two-dimensional metamaterial. The orientation of the lattice and the stripe direction are the same as those in Figure 1. At times before 2.4 s, only a dc bias was applied, and the DNA traveled mostly inside wide channel segments. At 2.4 s, an ac field (350 V/cm, 300 Hz) was added to the dc bias, and the polymer subsequently aligned with the narrow channels. The molecule then moved along the narrow channels.

the direction of the narrow channels, orthogonal to the previous direction, and proceeded to move along that axis. This effect is unique to the tailored energetic environment that the polymer experienced in our structure.

The fluidic network consists of a lattice of nanochannels that was patterned using electron beam lithography on a fused silica wafer, etched into the surface using reactive ion etching (RIE), and then sealed with a fused silica cover slip. Nanochannels formed a square lattice with a period of 2 μm and were about 100 nm deep. We successfully tested nanochannels of various widths between 80 and 140 nm but choose lattices with channel widths of 100 and 130 nm in the two principal directions of the array, respectively, for all data reported for asymmetric devices. The array extended over 200 μm $\times$ 128 μm. The short sides of the array were interfaced by microchannels 100 μm wide and 1 μm deep, prepared by optical lithography and RIE. The widths of the nanochannels were chosen so that DNA would be stretched to about 50% of its contour length.[4] Nanochannels were oriented at a 45° angle to the sides of the stripe.

A solution containing λ-DNA (16.5 μm contour length, New England Biolabs, Ipswich, MA) was introduced into the system, and DNA was visualized by epifluorescence of the bisintercalating dye YOYO-1 (Invitrogen, Carlsbad, CA) under 488 nm laser excitation using an intensified CCD camera (Princeton Instruments, Lawrence, NJ) and a fluorescence microscope (Nikon Instruments, Melville, NY). The dye-to-basepair ratio was 1:10, and the DNA was suspended in a 0.5 $\times$ TBE buffer solution. Photobleaching was slowed by adding an oxygen scavenging system containing glucose oxidase, catalase, β-D-(+)-glucose, and 2-mercaptoethanol. Electroendoosmosis was suppressed by adding 0.1 wt % of POP6 (Applied Biosystems, Foster City, CA). DNA was moved through the device using a voltage applied by platinum electrodes placed into reservoirs at the ends of the microchannels, about 6 mm away from the nanochannel lattice. The voltages were adjusted so that a homogeneous external field was applied parallel to the long side of the nanochannel array.[12]

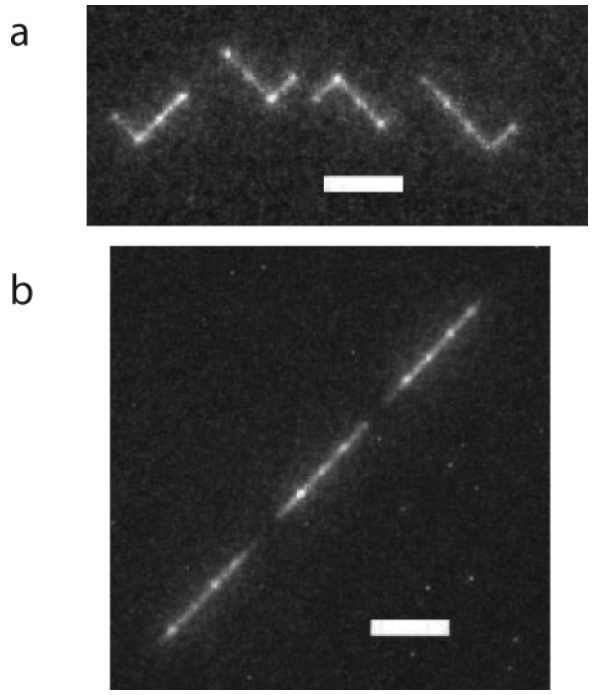

Figure 3. Movement of λ-DNA in lattices without an ac field. To show multiple configurations of the same molecule, a small dc bias was applied in both cases. (a) Movement in a symmetric square lattice of 100 nm wide nanochannels (scale bar 5 μm, frame spacing 8 s). The molecule has no preference for occupying a particular direction, and the ratio of straight to kinked geometries at junctions is about 1. (b) Movement in an asymmetric lattice (scale bar 5 μm, frame spacing 1.5 s). The molecule is completely confined inside wide channels.

We can understand the effect of an asymmetric lattice in the absence of an applied electric field by considering the free energy of confinement U_S.[11] For use with a single nanochannel segment in a lattice, we rewrite de Gennes' result[1,13] in terms of the occupied length along the channel, L_z, which is set equal to the lattice constant

$$U_S \cong k_B T \frac{L_z}{D} \tag{1}$$

D is the width of the nanochannel, which can be replaced by the geometric average of width and height for rectangular channels. Remarkably, this relationship is independent of the structural details of the polymer, except for that the molecule has to be long enough to be treated as linearized inside the nanochannel segment. Note that U_S is of direct importance to the configuration of molecules in an asymmetric lattice, as it acts to drive DNA from narrow channels into wider channels.

The effect of U_S is illustrated in Figure 3, which shows DNA molecules in a symmetric and an asymmetric lattice, respectively. In the symmetric lattice (Figure 3a), the molecule formed kinked and straight conformations at junctions with about equal probability. On average, the molecule had no preferred orientation. In contrast to the symmetric lattice, an asymmetric structure (Figure 3b) did result in almost exclusively straight configurations at channel

junctions. More specifically, we observed that the molecule was contained within the wider channels, in agreement with the functional dependence of U_S on D. Molecules thus exhibited a net alignment.

Interestingly, the average migration direction of molecules under dc electrophoresis mirrored the alignment within both symmetric and asymmetric devices. On average, DNA moved parallel to the stripe direction (horizontal) in the symmetric structure and at a 45° angle to that in the asymmetric lattice. An asymmetric material thus remarkably leads to polymer transport that is not parallel to the average current density. Note that the entropic effect described here is substantially different from size-dependent sorting,[14] since DNA has no local intrinsic size, and the phenomenon is independent of DNA length.

We can estimate the effectiveness of alignment in the asymmetric lattice by using a Boltzmann relationship and eq 1. For the structure presented in Figure 3, we conclude that the fraction of narrow channel segments out of all occupied segments should be about 8%. This fraction is roughly consistent with the experimental value of at most 10% that was observed using molecules with a drift velocity equal to or less than 2 μm/s.

We now consider a device with an applied ac voltage. The periodic polarization of the counterion cloud surrounding the DNA leads to an attractive dielectrophoretic potential U_E that is proportional to the square of the electric field.[15] An intuitive understanding of the electric field distribution inside the device can be obtained by the following Gedankenexperiment. We consider an infinitely long stripe of the metamaterial that has a finite width. Let us initially also assume that the electric field strength inside wide and narrow channels is equal. Since the resistance of the wide channels is lower than the one of the narrow channels, the current through wide channels is larger than that through narrow channels, and the combined average current flows not parallel to the stripe, but at an angle to it. The current component perpendicular to the stripe would however charge the insulating boundaries, and that charge would give rise to an electric field component perpendicular to the stripe. To reach steady state, the charging has to cease, and that is exactly the case when the current is parallel to the stripe, with no perpendicular component. At that point an equal current has to flow through narrow and wide channels. Given equal buffer conductivity but different cross sections of narrow and wide nanochannels, that in turn requires that the local field strengths inside the nanochannels are inversely proportional to their cross sections. A detailed numerical calculation of the electric fields (Figure 4a) assuming equal total currents through narrow and wide channels confirms this simple argument but shows some added complexity at channel junction. We have also tested whether the assumption of an infinitely long stripe holds for our geometry using a mean-field model with an anisotropic conductivity and found a satisfactory agreement with the above argument in the center of the device and close to the insulating walls.

Because of the distribution of the electric field strength and functional dependence of the dielectrophoretic potential

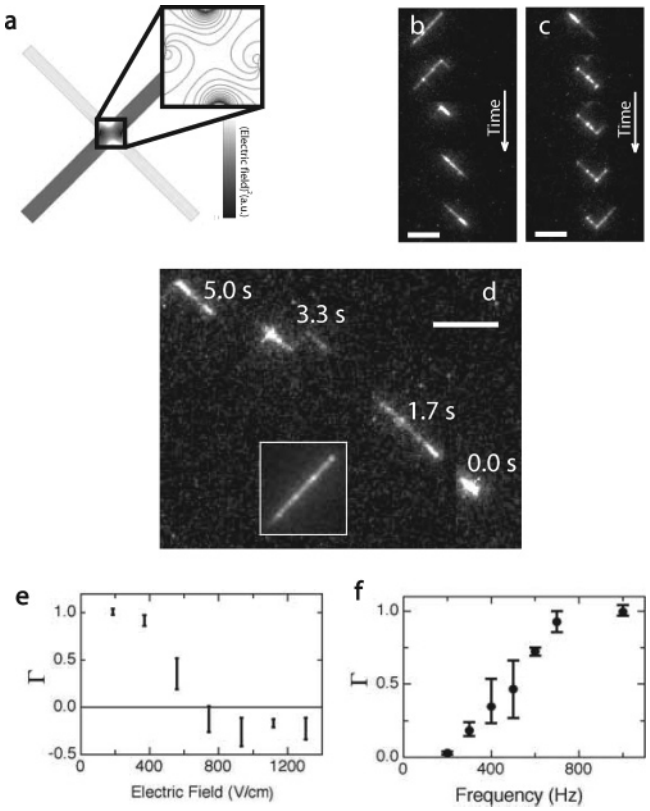

Figure 4. Alignment of DNA under an ac field. (a) Electric fields squared in the unit cell of a square lattice with 100 nm and 140 nm wide nanochannels, in arbitrary units, calculated using FEMLab (Comsol, Burlington, MA). The inset shows lines of equal potential energy due to dielectrophoresis close the nanochannel junction. (b) DNA moving from wide into narrow channels of an asymmetric lattice as an ac voltage is applied in the second frame (frame spacing 650 ms, scale bar 5 μm). (c) DNA relaxing into wide nanochannel after removal of the ac voltage (frame spacing 2.6 s, scale bar 5 μm). (d) Molecule moving through an asymmetric array in the presence of an ac field with a dc offset (exposure time 0.55 s, frame spacing 1.65 s, scale bar is 5 μm). The DNA is aligned with the narrow channels and moves by hopping between narrow segments. The inset shows the same molecule before applying any voltage and aligned with the wide channels. (e) Alignment coefficient Γ for a λ-DNA molecule in a lattice with 100 nm and 130 nm wide nanochannels as a function of the applied ac electric field at a frequency of 1 kHz. Positive values signify alignment along the direction of the wide channels and negative ones alignment along the direction of the narrow channels. Bars indicate minima and maxima over all measurements. (f) Alignment coefficient Γ for a λ-DNA dimer vs frequency at an ac field strength of 200 V/cm.

U_E on it, U_E will counteract the free energy of confinement U_S and drive DNA into narrower channel segments. On average, a high-strength ac electric field will orient DNA along the narrow channels. To rephrase the result, we are able to tune the strength of the confinement potential to the point of reversing the sign of the net force by applying ac electric fields.

We demonstrate the effect of an ac field in parts b and c of Figure 4, using the same device as in Figure 3b. Upon application of the ac voltage, the molecule rapidly moved from wide channel segments into a narrow segment and contracted at the same time. When the ac voltage was turned off, a slow relaxation back into a wide channel followed.

We then added a dc offset to the ac voltage and observed movement of DNA along the narrow channels, with occasional lane skips (Figure 4d). The motion occurs not homogeneously, but rather in jumps. We can explain this by the pinning of DNA at junctions due to the local minima of the entropic and dielectrophoretic potentials there.

A few points about DNA confinement in an ac electric field merit further attention. We quantified the effect of the ac voltage and frequency by calculating the alignment coefficient Γ, which is defined in the following (Figure 4). Γ is based on the average spatial two-dimensional fast Fourier transform (FFT) for a molecule over all frames of a movie. We took the difference between the components in the principal directions divided by the total intensity in the Fourier transform along the two axes. For each molecule we calculated this ratio with and without ac field, and the ratio of those is the alignment coefficient Γ. Positive values signify alignment along the direction of the wide channels, and negative ones alignment along the direction of the narrow channels.

The graph of Γ as a function of the applied ac voltage exhibits the signature of a phase transition with a transition point from alignment in wide channels to alignment in narrow channels at around 600 V/cm. When the frequency of the ac field was varied between 200 Hz and 1 kHz at a constant ac voltage, we found that the alignment in narrow channels decreased as the frequency was increased. Both observations are in agreement with the treatment presented by Chou et al.,[15] who describe the dielectric response as arising from the polarization and relaxation of the counterion cloud around a polyelectrolyte in a salt solution. However, the precise mechanism may be more intricate since for nanoconfined DNA the interaction of counterions, channel walls, and DNA may become inextricably linked. Note that in Figure 4, Γ did not fully reverse sign for the following reasons. (A) DNA gets compressed, and especially at very high voltages DNA is concentrated at nodes. (B) Because of the electric field distribution at junctions, kinked configurations are preferred over straight ones at very high fields. We observed that the contraction of DNA under an ac field can be divided into two distinct phenomena, which are the attractive nature of junctions, and the condensation of DNA under high electric fields. The latter appears to be a universal phenomenon resembling a phase transition, which was also observed in straight, unbranched nanochannels.

While all the observations reported in this work were obtained using double-stranded DNA, the results are expected to hold in a more general sense as outlined in the following. All semiflexible, self-excluding polymers are expected to align in an asymmetric matrix, given that the polymer strands are long enough to fill a full period of the lattice. Polymer transport can occur by fluid flow, or any other mechanism such as electrophoresis. The electrical switching of the anisotropy is dependent on the ac response of the polymer, but we expect the basic behavior to be maintained for all polyelectrolytes.

We also expect that many of the conceptual elements introduced in this paper will become important in the operation of complex nanofluidic systems. The key concepts are junctions of nanochannels, asymmetric junctions and their impact on polymer transport, especially the ability to confine DNA in wide channels while exposing the junctions to a perpendicular electrokinetic flow, and the manipulation of DNA inside nanochannels using a tunable combined entropic/dielectrophoric potential landscape. Using these concepts, targeted, pointlike DNA modification, switches linking different nanofluidic stages, molecule sorters and other new functional elements for biological and biopolymer analysis become feasible.

Acknowledgment. We thank Walter Reisner and Shuang Fang Lim for insightful discussions. This work was supported by grants from DARPA (MDA972-00-1-0031), NIH (HG0-1506), and the NSF Nanobiology Technology Center (BSCECS9876771). Part of the work was performed at the Cornell Nano-Scale Science and Technology Facility (CNF) which is supported by the National Science Foundation under Grant No. ECS-973129.

References

(1) de Gennes, P. G. *Scaling Concepts in Polymer Physics*; Cornell University Press: Ithaca, NY, 1979.
(2) Doi, M.; Edwards, S. *The Theory of Polymer Dynamics*; Oxford University Press: Oxford, U.K., 1986.
(3) Turner, S. W.; Perez, A. M.; Lopez, A.; Craighead, H. G. *J. Vac. Sci. Technol., B* **1998**, *16*, 3835−3840.
(4) Tegenfeldt, J. O.; Prinz, C.; Cao, H.; Chou, S.; Reisner, W. W.; Riehn, R.; Wang, Y. M.; Cox, E. C.; Sturm, J. C.; Silberzan, P.; Austin, R. H. *Proc. Natl. Acad. Sci. U.S.A.* **2004**, *101*, 10979−10983.
(5) Nykypanchuk, D.; Strey, H. H.; Hoagland, D. A. *Science* **2002**, *297*, 987−990.
(6) Fan, R.; Karnik, R.; Yue, M.; Li, D. Y.; Majumdar, A.; Yang, P. D. *Nano Lett.* **2005**, *5*, 1633−1637.
(7) Volkmuth, W. D.; Austin, R. H. *Nature* **1992**, *358*, 600−602.
(8) Han, J.; Craighead, H. G. *Science* **2000**, *288*, 1026−1029.
(9) Turner, S. W. P.; Cabodi, M.; Craighead, H. G. *Phys. Rev. Lett.* **2002**, *88*, 128103.
(10) Pockels, F. *Lehrbuch der Kristalloptik.*; Teubner Verlag: Leipzig, Germany, 1906.
(11) Reisner, W.; Morton, K. J.; Riehn, R.; Wang, Y. M.; Yu, Z.; Rosen, M.; Sturm, J. C.; Chou, S. Y.; Frey, E.; Austin, R. H. *Phys. Rev. Lett.* **2005**, *94*, 196101.
(12) Riehn, R.; Lu, M.; Wang, Y. M.; Lim, S. F.; Cox, E. C.; Austin, R. H. *Proc. Natl. Acad. Sci. U.S.A.* **2005**, *102*, 10012−10016.
(13) Schaefer, D. W.; Joanny, J. F.; Pincus, P. *Macromolecules* **1980**, *13*, 1280−1289.
(14) Huang, L. R.; Cox, E. C.; Austin, R. H.; Sturm, J. C. *Science* **2004**, *304*, 987−990.
(15) Chou, C. F.; Tegenfeldt, J. O.; Bakajin, O.; Chan, S. S.; Cox, E. C.; Darnton, N.; Duke, T.; Austin, R. H. *Biophys. J.* **2002**, *83*, 2170−2179.

NL061137B